POAC'11
POAC11-022 Montréal, Canada

Proceedings of the 21st International Conference on
Port and Ocean Engineering under Arctic Conditions
July 10-14, 2011
Montréal, Canada

PHENOMENA BEHIND PEAK LOADS ON INCLINED STRUCTURE DURING A SIMULATED ICE PILE-UP PROCESS

Jani Paavilainen*, Jukka Tuhkuri and Arttu Polojärvi
Aalto University, School of Engineering, Espoo, FINLAND

ABSTRACT

This paper examines peak load phenomena during an ice pile build-up process against an inclined structure by simulating the process with a two dimensional combined finite discrete element method. In the method used, the level ice sheet and its fracture are modelled by using a finite element scheme, while the contact forces between the colliding ice blocks are calculated by using the discrete element method. A total of 28 peak load cases are studied and the phenomena during these peak load events are described. Peak loads are noticed to occur in the cases of ice ride-up, formation of a sail in front or away from the structure, and loading through a rubble pile. The common phenomenon of the four peak load situations was loading of the rubble pile in such a manner that the whole pile or a part of the pile was pushed upwards.

INTRODUCTION

The failure of an ice sheet against an inclined structure is a process where an initially intact ice sheet breaks into discrete ice blocks which then accumulate in the ice-structure interface and thus affect the failure process. The understanding of this fragmentation process and the calculation of the ice load on structure are important challenges. According to Brown et al. (2010), one event that is assumed to cause extreme ice loads on an offshore structure is a build-up of a large rubble pile on the structure. To be able to get an exact view of this extreme ice load event, the phenomena that are behind it should be understood. This is possible by simulating the processes and analyzing the results carefully. These rubble pile build-up simulations have previously been done by e.g. Hopkins (1997) and Paavilainen et al. (2006).

This paper examines ice sheet failure against a wide inclined structure by simulating the process with a two dimensional combined finite discrete element method. First, the paper presents assumptions made in the numerical method and the simulation set-up, including parameters of the simulations. Next, comparisons of the simulated process and loads are made with full scale experiments. Nine representative simulations are chosen for a detailed study. Finally, the results of these representative simulations concerning phenomena during peak loads in the inclined structure are presented.

*Corresponding author. *E-mail address:* jani.paavilainen@aalto.fi

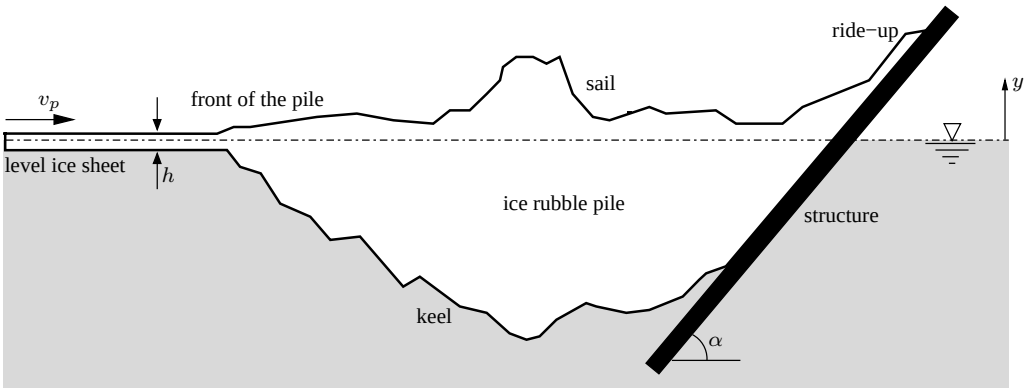

Figure 1: Schematic figure of ice rubble pile and the inclined structure.

2D ICE PILE-UP SIMULATIONS

The ice rubble formation process was simulated by using a two dimensional combined finite-discrete element method. The method can be divided into three main parts: i) continuum, ii) failure and iii) contact model. The forces obtained from these three parts are used in Newton's equations of motion, which are solved with an explicit time integration scheme. A comprehensive presentation of the method can be found in Paavilainen et al. (2009).

In the simulations, it was assumed that there is no freezing between the ice blocks in the rubble. Therefore, only loose ice rubble can be modelled, which is assumed to be the case during a rubble formation process. Another limiting assumption deals with the compressive failure of ice. The ice sheet failure modes accounted for in the simulations were bending, shear, buckling and crushing in contact areas. However, a compressive failure does not change the ice block geometry or create new ice features. This limits the use of vertical or near vertical structures in simulations. It was further assumed that no grounding of the rubble occurs and, since the method is two dimensional, no clearing of ice around the structure happens. Water induced effects accounted for in the simulations were buoyancy and drag force.

In the simulations, a floating ice sheet was pushed at its left end with a constant velocity v_p against a wide infinitely rigid inclined structure, as shown in Figure 1. The inclination angle of the structure was α, measured from the horizonal. In the left end of the ice sheet, about 100 m from the structure, a viscous damping boundary condition was applied. In simulations, initial velocities were $\dot{\mathbf{x}}_0 = \mathbf{0}$ m/s and the velocity at the leftmost element increased linearly from zero to v_p during time $t = [0, 1]$ s.

Table 1 lists the values of the parameters used in the simulations. The main parameters of the simulations were level ice thickness h and friction between the ice blocks μ_{ii}. The damping constants for both internal c_i and contact c_c damping were defined to have the value of the critical damping. The shear modulus G was defined by using Young's modulus E and Poisson ratio ν as $G = \frac{E}{2(1+\nu)}$. The fracture energy of ice G_f used in the simulations was based on the work of Dempsey et al. (1999). The tensile strength σ_f and the shear strength τ_f were used as the critical values in the fracture criterion. Shear strength was defined to be proportional to the tensile strength by $\tau_f = 0.65\sigma_f$. The value for the plastic limit σ_p used in the contact model was obtained from (Timco and Frederking, 1990). Values for ice–ice friction μ_{ii} are reported by Timco and Weeks (2010) and Lishman et al. (2009). Since the ice–ice friction is

Table 1: Parameters used in simulations.

	Parameter	Symbol	Unit	Value
General	Time step	Δt	s	$2.0 \cdot 10^{-5}$
	Ice sheet velocity	v_p	m s^{-1}	0.05
	Element length	L_0	m	0.25, 0.5
	Drag coefficient	d_c		2.0
Ice	Thickness	h	m	0.25 ... 1.25
	Young's modulus	E	GPa	4.0
	Poisson ratio	ν		0.3
	Density	ρ_i	kg m^{-3}	900
	Tensile strength	σ_f	kPa	400
	Fracture energy	G_f	J m^{-2}	12
Contact	Normal stiffness	k_{ne}	GPa	4.0
	Tangential stiffness	k_{te}	GPa	1.5
	Plastic limit	σ_p	MPa	2.0
	Ice–ice friction	μ_{ii}		0.01, 0.10, 0.35, 0.55
	Ice–structure friction	μ_{is}		0.10, 0.15
Water	Density	ρ_w	kg m^{-3}	1010
Structure	Inclination angle	α	$^\circ$	50, 82

heavily dependent on the prevailing condition, a wide range of friction was used to observe the influence of friction on the process.

A schematic picture of ice rubble pile is presented in Figure 1. The figure shows keel and sail parts of the rubble pile and also the level ice sheet that is pushed to the pile from the front of the pile. The ice ride-up along the structure is also sketched in the figure.

In the simulations, the rubble pile formation process was continued for such a long time that most of the process events are assumed to have occurred. This is supported by the fact that all the observed process phenomena repeated themselves in different simulations. Therefore, it is possible to analyse the phenomena behind these different events in detail. In this paper, nine simulations, identified with numbers $11 - 19$, are analysed in depth. The main parameters of these representative simulations are given in Table 2, and the other parameters are as shown in Table 1. First, however, the simulated process is compared with full-scale field measurements.

COMPARISON WITH FIELD MEASUREMENTS

As the simulations model ice sheet failure in two dimensions, the results are best compared with a wide structure, such as the Molikpaq. The Molikpaq is a steel caisson with octagonal shape consisting of four 60 m long sides and four 22 m long sides. At the mean water level, the Molikpaq has a diameter of 90 m and angle of outer face $\alpha = 82^\circ$. Full scale observations from the Molikpaq have been reported by Neth (1991) and Timco and Johnston (2003, 2004).

Level ice was observed to fail against the Molikpaq through crushing, bending, mixed mode, and creep. In crushing, ice fragmented into a large number of small pieces, while bending failure resulted into larger ice pieces. Mixed mode failures included crushing, bending and splitting of ice floes. Creep refers to a failure mode with a long loading time and no visible ice movement. In several occasions, a rubble pile formed along the Molikpaq. Creep, floe splitting or high speed impacts of isolated floes were unlikely to result into rubble piles, while crushing

Table 2: Main parameters of the nine representative simulations.

Id	h [m]	α [°]	μ_{ii}	μ_{is}	L_0 [m]
11	0.25	50	0.35	0.10	0.25
12	0.50	50	0.35	0.10	0.50
13	0.75	50	0.35	0.10	0.50
14	0.925	50	0.35	0.10	0.50
15	1.25	50	0.35	0.10	0.50
16	0.50	50	0.01	0.15	0.50
17	0.50	50	0.10	0.15	0.50
18	0.50	50	0.35	0.15	0.50
19	0.50	50	0.55	0.15	0.50

and bending failures were more likely to generate rubble. Both floating and grounded rubble piles were observed.

Qualitatively, the simulations agree well with the observed rubble formation against the Molikpaq. Both in simulations and in full scale, there was upward and downward bending failures, formation of ice blocks, ride-ups, and sails in front of the structure. In addition, as the pile had formed, ice sheet failed by bending also against the pile, away from the structure.

Of the different first year level ice failure modes observed at the Molikpaq, the current simulation method can best model bending or mixed mode failures leading to formation of floating rubble piles. A table by Timco and Johnston (2004) includes data from 12 mixed mode events leading to rubble formation, and 14 rubble formation events whose primary mode is not known. Data of these 26 events is shown Figure 2, and is used here to compare with the simulation results. Following Timco and Johnston (2003), the full scale loads are given as Line Loads defined as

$$\text{Line Load} = \frac{\text{Measured Global Load}}{\text{Width of Structure loaded by the Ice}} \, .$$

Line Loads defined this way can be directly compared to simulated two dimensional loads.

Four simulations with different ice thicknesses (0.75 m, 0.9 m, 1.0 m, and 1.1 m) were conducted to model rubble formation against the Molikpaq. In these simulations, the inclination angle of the structure was $\alpha = 82°$, the frictions were $\mu_{ii} = 0.35$, $\mu_{is} = 0.1$, and the element length was $L_0 = 0.5$ m. Other parameters were as shown in Table 1.

For the simulation method used, the inclination angle 82° is steep because crushing of the level ice sheet was modelled only through a plastic limit. However, as reported by Neth (1991), during a mixed mode event, extensive ride-up and flexural failure were observed also at the rubble edge and not only at the structure. Therefore, ice loads from the later parts of the simulation, when a rubble pile already had formed, are used in this comparison with full scale data.

Figure 2 shows the measured and simulated peak loads on the Molikpaq caused by rubble formation with different ice thicknesses. The simulation method models rather well these events. Especially, the measured and simulated loads on mixed mode cases with thick ice are similar. The failure mode was unknown at the events with $h = 0.7$ m, and these events could thus

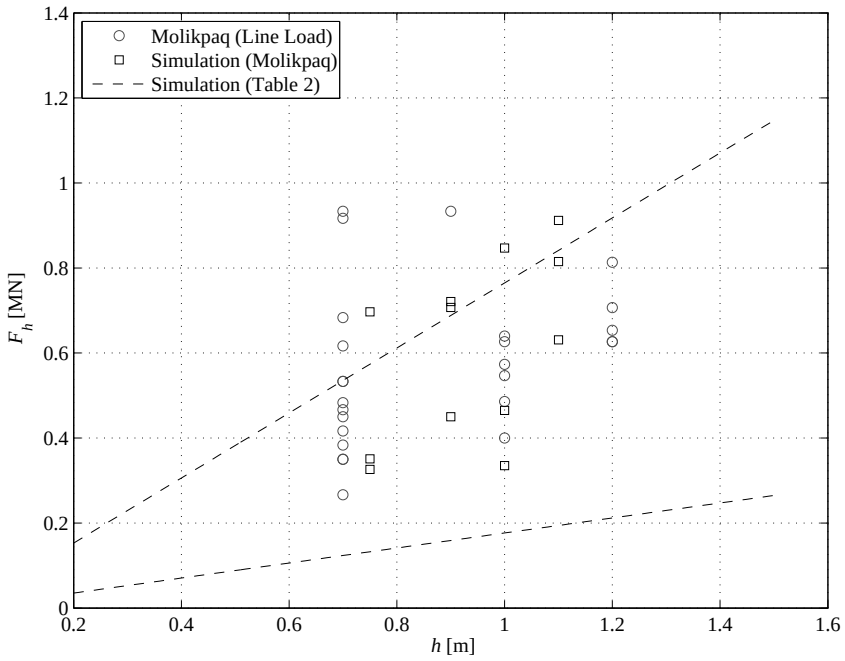

Figure 2: Full-scale peak Line Load measured from Molikpaq (Timco and Johnston, 2004) and simulated peak loads as functions of ice thickness. Also, the limiting lines for the peak loads from the simulations with inclination angle $\alpha = 50°$ listed in Table 2 are shown.

include both crushing with high loads and mixed mode failure with lower loads.

Figure 2 shows also with two lines the range of peak loads obtained from the simulations listed in Table 2. As these loads are from simulations with inclination angle $\alpha = 50°$, they are understandably lower than those on the Molikpaq, but the difference is not major.

The simulations were also able to capture the force-displacement record of the process reasonably well. The force-displacement records, as illustrated in Figure 3, show very similar behavior as has been seen in the full scale measurements (Neth, 1991; Timco and Johnston, 2003). First the force increases followed by a more or less sudden decrease of the force. This cycle then repeats itself many times during the process.

PHENOMENA DURING PEAK LOADS ON THE STRUCTURE

From each of the nine simulations in Table 2, three peak load events were chosen, as shown e.g. in Figure 3. Of the three force peaks, one was from the initial, one from the middle and one from the final stage of a simulation. These peak load events are termed as 1, 2 and 3, respectively. For the simulation with Id 12, also one additional force peak referred as 2^* was chosen. The selected 28 extreme events were analysed in more detail. In particular, different situations leading to the force peaks and also the reasons that lead to decrease of the force peaks were addressed.

One situation leading to a peak load is the ride-up of an ice sheet on the structure. An example of a ride-up is the event 1 in simulation with Id $= 13$. A close up of the force during this case is shown in Figure 4. In Figure 5, nondimensional average velocities v/v_p of discrete elements

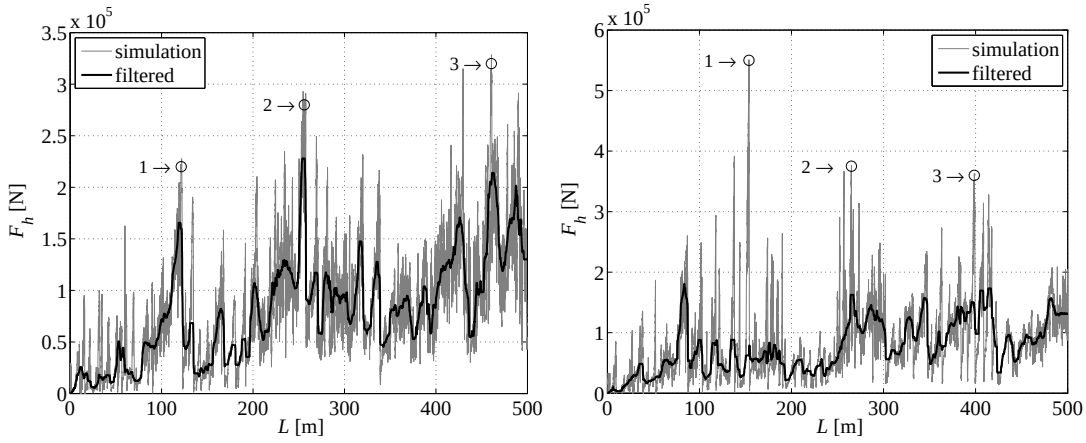

(a) Simulation Id 13, $h = 0.75$ m. (b) Simulation Id 14, $h = 0.925$ m.

Figure 3: Horizontal force F_h acting on the structure as a function of the length of the pushed ice L for simulations with Ids 13 and 14. Both the original and median filtered force are presented. The numbers $\{1, 2, 3\}$ refer to chosen peak forces.

in the ice rubble during a time interval δt are shown. During $L = 110 - 121$ m the ice sheet is gradually riding up and some minor load drops can be seen from Figure 4. It can be noticed that the load is increasing as long as the pile below the pushing ice sheet is being pushed up the structure, see Figs 4, and 5a. As the rubble pile under the pushing sheet stops, the load no longer increases, even though the level ice sheet is still moving upwards along the structure, Figs. 4, 5b. The major load drop at $L = 122.5 - 123.0$ m is due collapse of the rubble pile, where major change in the pile geometry occurred and the level ice riding up slip downwards to water.

In addition to ride-up (RU, Figure 5), other peak load events observed in the simulations involve loading through rubble pile (LRP), formation of sails away from the structure (SAFS), and formation of sails in front of the structure (SIFS). These events are presented more closely in (Paavilainen et al., 2011). In SIFS and SAFS, a sail can clearly be observed and an ice sheet having an even surface is pushed to that sail. In LRP, the ice sheet is not clearly pushing the sail, or no sail can be observed between the structure and the pushing ice sheet.

The reasons for the major load drops are hard to identify unambiguously for all the cases. The major load drops usually involve some sort of change in the rubble configuration. This change can involve many individual events, so it is difficult to distinguish which one of them is the main reason. Therefore, only the following broad definitions for the major load drops are used: sail failure or deformation (SFD), rubble failure (RF), and pushing ice sheet failure (PIF). Examples of these cases are given in (Paavilainen et al., 2011).

The events behind the peak load cases and the reasons for the major load drops in the simulations with different ice thicknesses and friction coefficients are collected to Tables 3 and 4. The symbols 1, 2, 2^* and 3 in Tables 3 and 4 refer to the representative events such as shown in Figure 3.

No clear effect of ice sheet thickness on the peak load cases or the major load drops can be noticed from Table 3. There is some indication, that with thin ice the peak load cases are due to sail formation, and that with thick ice the peak load cases are due to ride-up and loading

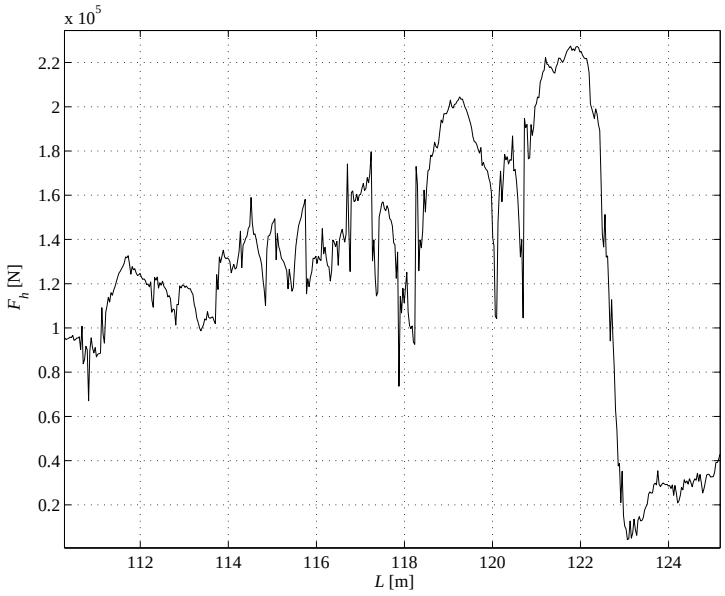

Figure 4: Horizontal force during an extreme event 1 in simulation with Id $= 13$, i.e. a close up of a horizontal force graph shown in Figure 3a.

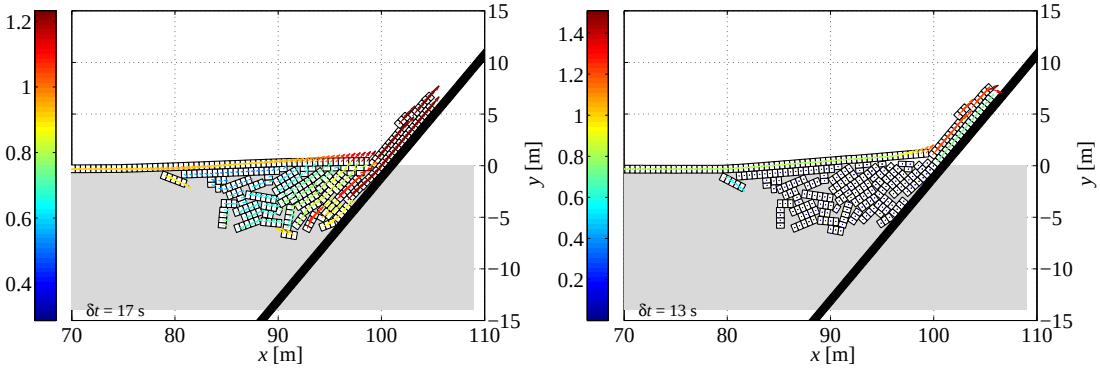

(a) Normalized velocity, $L = 120.9$ m.

(b) Normalized velocity, $L = 121.8$ m.

Figure 5: Ice rubble pile during an extreme event 1 in simulation with Id $= 13$. The horizontal force during this event is shown in Figure 4. a) Force increasing as pile is pushed to structure with the ride-up. b) Rubble pile stops and ride-up moving upwards. Force on the structure decreasing, see Figure 4. Scale not constant between the plots.

through a rubble pile, but the effect of ice thickness on rubble formation processes requires further studies.

From Table 4 it can be observed that with low ice–ice frictions $\mu_{ii} = 0.01 - 0.10$, the peak forces are due to ride-ups or loadings through rubble piles. By looking closer at these cases, it was noticed that such sails that could be pushed by the ice sheet did not form. With low friction, the sails were low (Paavilainen et al., 2010). There were sails, but they were formed from deforming rubble rather than directly from the pushing ice sheet. On the other hand, with higher ice–ice frictions $\mu_{ii} = 0.35 - 0.55$, peak loads occur when ice sheet is loading the structure through a rubble pile or through a sail formed away from the structure.

Table 3: Events behind the peak loads and reasons for the major load drops with different ice thicknesses h for simulations with Ids $11-15$ ($\mu_{ii}=0.35$). The symbols 1, 2, 2^* and 3 indicate the representative extreme events (see e.g. Figure 3). Abbreviations for peak loads: RU$\equiv$ ride-up, SIFS $\equiv$ sail in front of structure, SAFS $\equiv$ sail away from structure and LRP $\equiv$ loading through rubble pile. Abbreviations for load drops: SFD$\equiv$ sail failure or deformation, RF $\equiv$ rubble failure, PIF $\equiv$ pushing ice sheet failure.

	Peak loads				Major load drops		
h [m]	RU	SIFS	SAFS	LRP	SFD	RF	PIF
0.25	–	1	2,3	–	2,3	1	–
0.50	–	1	2,2*	3	–	2*	1,2,3
0.75	1	2	3	–	3	1,2	–
0.925	–	–	2	1,3	2	–	1,3
1.25	1,3	–	–	2	–	1	2,3

Table 4: Events behind the peak loads and reasons for the major load drops with different ice-ice frictions μ_{ii} for simulations with Ids $16-19$ ($h=0.5$ m). The symbols 1,2 and 3 indicate the representative extreme events. Abbreviations for peak loads: RU$\equiv$ ride-up, SIFS $\equiv$ sail in front of structure, SAFS $\equiv$ sail away from structure and LRP $\equiv$ loading through rubble pile. Abbreviations for load drops: SFD$\equiv$ sail failure or deformation, RF $\equiv$ rubble failure, PIF $\equiv$ pushing ice sheet failure.

	Peak loads				Major load drops		
μ_{ii}	RU	SIFS	SAFS	LRP	SFD	RF	PIF
0.01	1	–	–	2,3	–	1,2,3	–
0.10	1,2	–	–	3	–	1,3	2
0.35	–	–	2	1,3	2	–	1,3
0.55	–	–	1	2,3	–	–	1,2,3

Table 4 shows also that almost all major load drops with low ice–ice frictions are due to rubble pile failures, and with high frictions they are due to pushing ice sheet failures. This seems logical, with higher ice–ice frictions more load is needed to deform the rubble pile.

Remembering that the symbols 1, 2, and 3 in Tables 3 and 4 indicate the amount of ice pushed into the rubble (see e.g. Figure 3), it is observed that the ride-ups and sails in front of structure are mostly occurring in the early stages of the simulation when smaller rubble piles are present. On the other hand, when a rubble pile has grown larger, the pushing ice sheet does not reach the structure easily and the ice sheet is forced to fail away from the structure. The same observation has also been made in full-scale (Neth, 1991).

A common phenomenon of the different peak load situations was loading of the rubble pile in a way that a part of the pile was pushed upwards. This happened either away from the structure or against the structure. This kind of situations caused peak forces in all of the peak load events that were analysed.

CONCLUSIONS

The process of ice sheet failure and rubble formation against a wide inclined structure was simulated with a two dimensional combined finite discrete element method (2D FEM-DEM). The assumptions used and the simulation set-up including parameters of the simulation were presented.

Simulations of the rubble formation process were shown to capture processes that are observed during full-scale events. Also, the simulated force-displacement records showed similar behavior than those obtained in full scale measurements. In addition, the peak loads were similar with those measured from the Molikpaq.

Nine representative simulations were studied in more detail, and the phenomena during 28 peak load events were analysed. Peak loads were noticed to occur in the cases of ice ride-up, formation of a sail in front or away from the structure, and loading through a rubble pile. The common phenomenon in the peak load situations was loading of the rubble in a manner where a part of the rubble was pushed upwards. These situations caused peak forces in all the events studied.

The main reasons for major load drops were found to be failure or deformation in the rubble, and failure of the pushing ice sheet. No clear effect of ice sheet thickness on the peak load or load drop mechanisms was noticed. With low ice–ice friction, the peak forces were due to ride-up or loading through rubble piles. With high ice–ice frictions, peak loads occurred when the ice sheet was pushed into a rubble field or into a sail formed away from the structure. With high friction, more load was needed to deform the rubble. Further, the ice sheet did not reach the structure easily when large rubble piles were present.

ACKNOWLEDGEMENTS

The financial support from the Ministry of Education of Finland through the National Graduate School in Engineering Mechanics is gratefully acknowledged.

REFERENCES

Brown, T., Tibbo, J., Thipathi, D., Obert, K., and Shrestha, N. (2010). Extreme ice load events on the Confederation Bridge. *Cold Regions Science and Technology*, 60(1):1–14.

Dempsey, J., Adamson, R., and Mulmule, S. (1999). Scale effects on the in-situ tensile strength and fracture of ice. Part II: First-year sea ice at Resolute, N.W.T. *International Journal of Fracture*, 95:347–366.

Hopkins, M. (1997). Onshore ice pile-up: a comparison between experiments and simulations.

Cold Regions Science and Technology, 26(3):205–214.

Lishman, B., Sammonds, P., Feltham, D., and Wilchinsky, A. (2009). The rate- and state-dependence of sea ice friction. In *Proceedings of the 20th International Conference on Port and Ocean Engineering under Arctic Conditions*. POAC 09. (Electronic publication).

Neth, V. (1991). Ice rubble formation along the Molikpaq. In Muggeridge, D., Colbourne, D., and Muggeridge, H., editors, *11th International Conference on Port and Ocean Engineering under Arctic Conditions*, volume I, pages 241–258, St. John's, Canada.

Paavilainen, J., Tuhkuri, J., and Polojärvi, A. (2006). Discrete element simulation of ice pile-up agaist an inclined structure. In *IAHR 06 Proceedings of the 18th International Symposium on Ice*, volume 2, pages 177–184, Sapporo, Japan.

Paavilainen, J., Tuhkuri, J., and Polojärvi, A. (2009). 2d combined finite-discrete element method to model multi-fracture of beam structures. *Engineering Computations*, 26(6):578–598.

Paavilainen, J., Tuhkuri, J., and Polojärvi, A. (2010). Rubble pile formation against an inclined structure – analysis of simulation results. In *IAHR 10 Proceedings of the 20th International Symposium on Ice*, Lahti, Finland. IAHR. (Electronic publication).

Paavilainen, J., Tuhkuri, J., and Polojärvi, A. (2011). 2d numerical simulations of ice rubble formation process against an inclined structure. *Submitted to: Cold Regions Science and Technology*.

Timco, G. and Frederking, R. (1990). Compressive strength of sea ice sheets. *Cold Regions Science and Technology*, 17(3):227–240.

Timco, G. and Johnston, M. (2003). Ice loads on the Molikpaq in the Canadian Beaufort Sea. *Cold Regions Science and Technology*, 37:51–68.

Timco, G. and Johnston, M. (2004). Ice loads on the caisson structures in the Canadian Beaufort Sea. *Cold Regions Science and Technology*, 38:185–209.

Timco, G. and Weeks, W. (2010). A review of the engineering properties of sea ice. *Cold Regions Science and Technology*, 60(2):107–129.